APPENDIX D

REPORT OF DESIGN PANEL

CONTENTS

Part		Page
	APPENDIX D - REPORT OF DESIGN PANEL	
D1	TASK ASSIGNMENT	D-1
D2	PANEL ORGANIZATION	D-3
D3	REVIEW AND ANALYSIS	D-5
	SYSTEM DESCRIPTION	D-5
	ELECTRICAL SYSTEM CONFIGURATION AT TIME OF ACCIDENT	D-11
	STRUCTURAL EVALUATION OF THE OXYGEN TANK	D-13
	Materials and Welding	D-13
	Qualification Program	D-20
	FRACTURE MECHANICS	D-23
	Failure Modes	D-24
	Effectiveness of the Proof Test	D-25
	Possibility of Tank Failure During Apollo 13 Mission	D-30
	DYNAMIC TESTING	D-30
	Oxygen Tank Assembly Dynamic Testing	D-30
	Apollo CSM Acoustic and Vibration Test Program	D-31
	SHOCK TESTING	D-35
	INTERNAL COMPONENTS	D-35
	Quantity Gage	D-35
	Heaters	D-37

Part | Page

Fans D-41

Temperature Sensor D-43

Wiring D-43

Discussion D-48

COMPATIBILITY OF MATERIALS WITH OXYGEN D-48

Classification Methods D-49

Materials Internal to the Tank D-49

OTHER DESIGN AND SYSTEM CONSIDERATIONS D-59

Oxygen System Relief Valves D-59

Arrangement at Head of Tank D-61

Dome Assembly D-64

Filter D-70

Caution and Warning Provisions D-70

ABNORMAL EVENTS IN THE HISTORY OF THE OXYGEN TANK D-71

Oxygen "Shelf Drop" Incident D-71

Detanking at KSC D-72

Discussion D-74

RELATED SYSTEMS D-78

Pressure Vessels D-78

Line Components D-85

Low Pressure Oxygen Systems D-86

Electrical Power System--Batteries D-86

Part		Page
	Ground Support Equipment	D-86
	Certification	D-87
	Apollo J-Missions	D-87
	Lunar Module "Lifeboat"	D-87
	DISCUSSION	D-87
D4	SUMMARY	D-89
D5	REFERENCES	D-93

This page left blank intentionally.

PART D1

TASK ASSIGNMENT

The Design Panel was assigned the task of reviewing the design of the systems involved in the Apollo 13 accident, including their qualification history. The service history of the specific components flown on Apollo 13 was also to be examined from a design point of view to ascertain whether any abnormal usage experienced might have had a detrimental effect on the functional integrity of the components. The Panel was also charged with review of other spacecraft systems of similar design or function to ascertain whether they contained potential hazards. Finally, the Panel was to analyze, as required by the Board, proposed failure mechanisms to the extent necessary to support the theory of failure.

The Panel conducted its activities by reviewing design documentation and drawings, historical records, and test reports; analyzing data; examining specimens of hardware; and consulting with other Board Panels and with members of the Manned Spacecraft Center (MSC) Investigation Team and the contractors.

This page left blank intentionally.

PART D2

PANEL ORGANIZATION

Panel 3 was chaired by Dr. S. C. Himmel, Lewis Research Center, and the Board Monitor was Mr. V. L. Johnson, Office of Space Science and Applications, NASA Headquarters. Panels Members were:

Mr. W. F. Brown, Jr.
Lewis Research Center

Mr. R. N. Lindley
Office of Manned Space Flight
NASA Headquarters

Dr. W. R. Lucas
Marshall Space Flight Center

Mr. J. F. Saunders, Jr.
Office of Manned Space Flight
NASA Headquarters

Mr. R. C. Wells
Langley Research Center

Specific assignments covering such areas as materials selection, fracture mechanics, materials compatibility, failure mechanisms, related systems, and electrical systems were given to each Panel Member. All Panel Members participated in the preparation of this report.

This page left blank intentionally.

PART D3

REVIEW AND ANALYSIS

Early in the proceedings of the Board, it became evident that the failure was centered in the cryogenic oxygen subsystem of the electrical power system of the spacecraft, and, more specifically, in the no. 2 cryogenic oxygen tank. For this reason, detailed examinations of the Panel were limited to this subsystem. Interfacing systems were examined only to the extent required to understand the function of the oxygen system and/or to relate data from flight or test to the operation or design of the system.

In addition, the Panel had one of its members present at the deliberations of the MSC Panel on Related Systems which conducted reviews on other Apollo spacecraft pressurized systems.

SYSTEM DESCRIPTION

The cryogenic storage subsystem supplies reactants to the fuel cells that provide electric power for the spacecraft. The oxygen system also supplies metabolic oxygen for the crew, command module (CM) cabin pressurization, and the initial pressurization of the lunar module (LM). The cryogenic storage and fuel cell subsystems are located in bay 4 of the service module (SM). Figure D3-1 shows the geometric arrangement of these subsystems within this portion of the SM. The system comprises two oxygen tanks, two hydrogen tanks, and three fuel cells with their associated plumbing, control valves, regulators, pressure switches, and instrumentation.

The uppermost shelf contains the three fuel cells; the center shelf contains the two oxygen tanks, the oxygen system valve modules, the fuel cell oxygen valve module, and a ground service interface panel. The lower shelf contains the two hydrogen tanks, one above and one below the shelf, and a set of valve modules analagous in function to those of the oxygen system.

A description of these components is contained in Appendix A of the Board's report. Also provided are the operating and design parameters of the components, materials of construction, etc.

A schematic of the oxygen system is shown in figure D3-2. The ground service lines are capped off prior to flight. Figure D3-3 is a photograph of the panel showing the terminations of these lines. The two tanks and

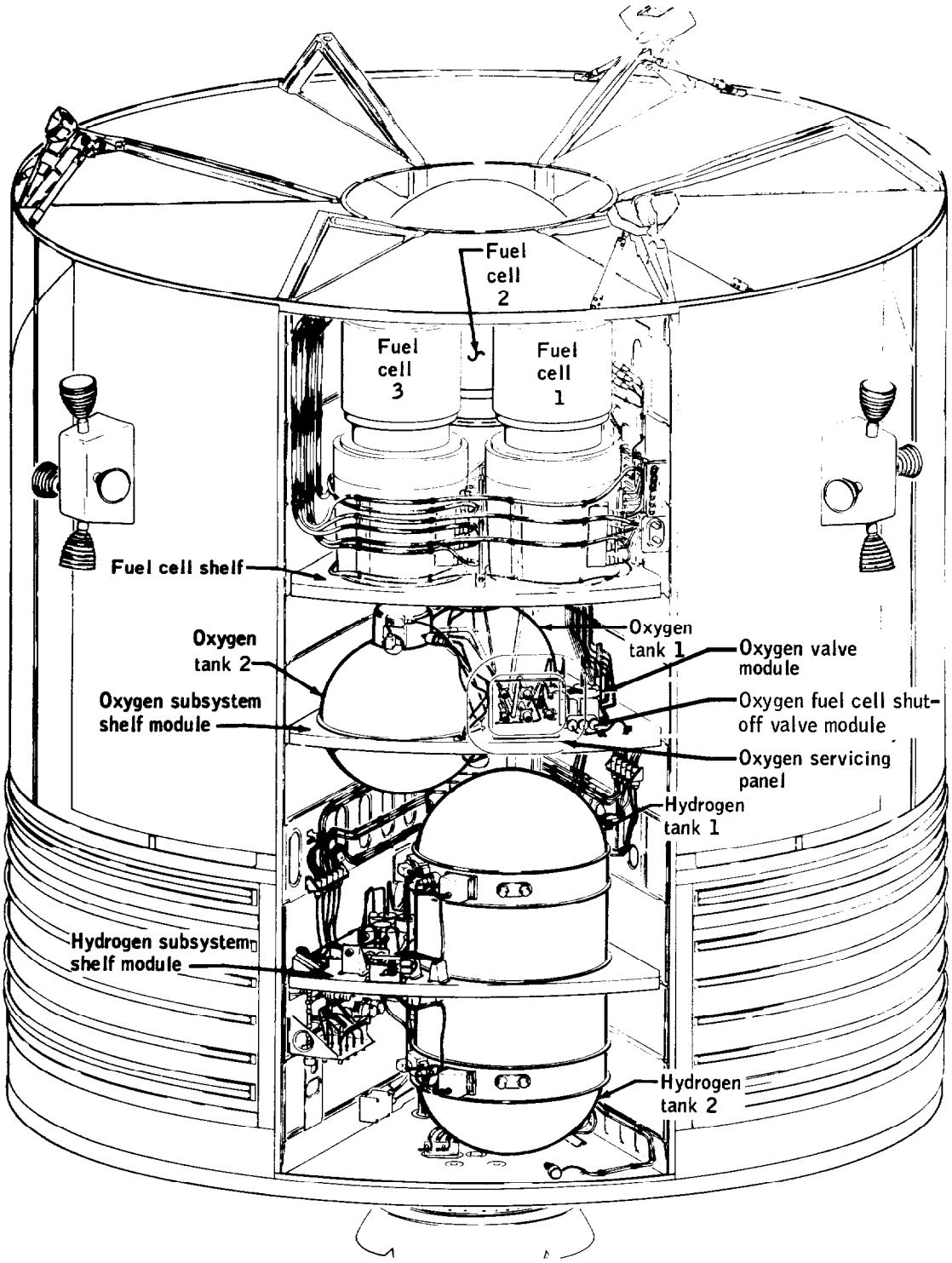

Figure D3-1.- Arrangement of fuel cells and cryogenic systems in bay 4.

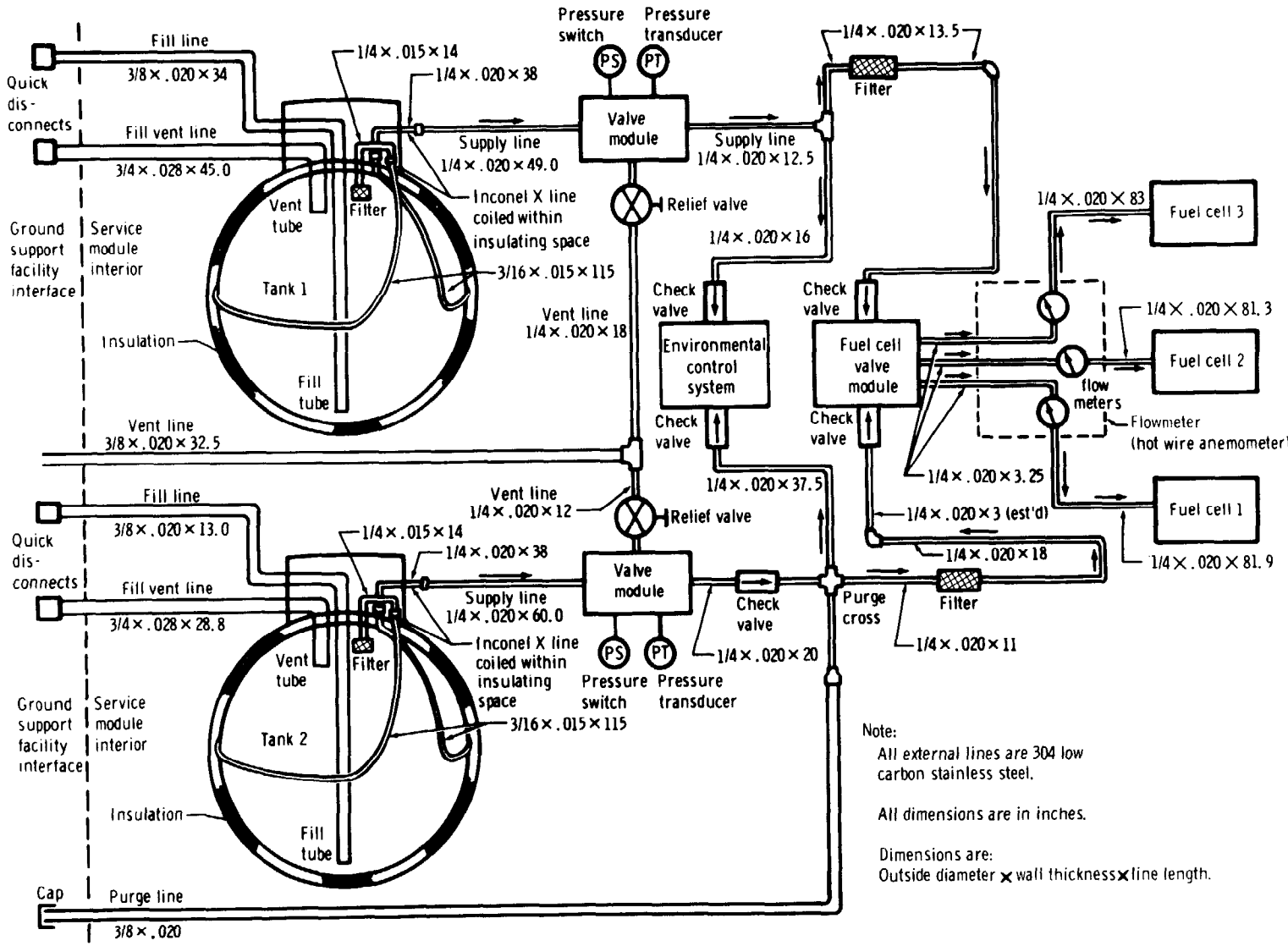

Figure D3-2.- Oxygen system.

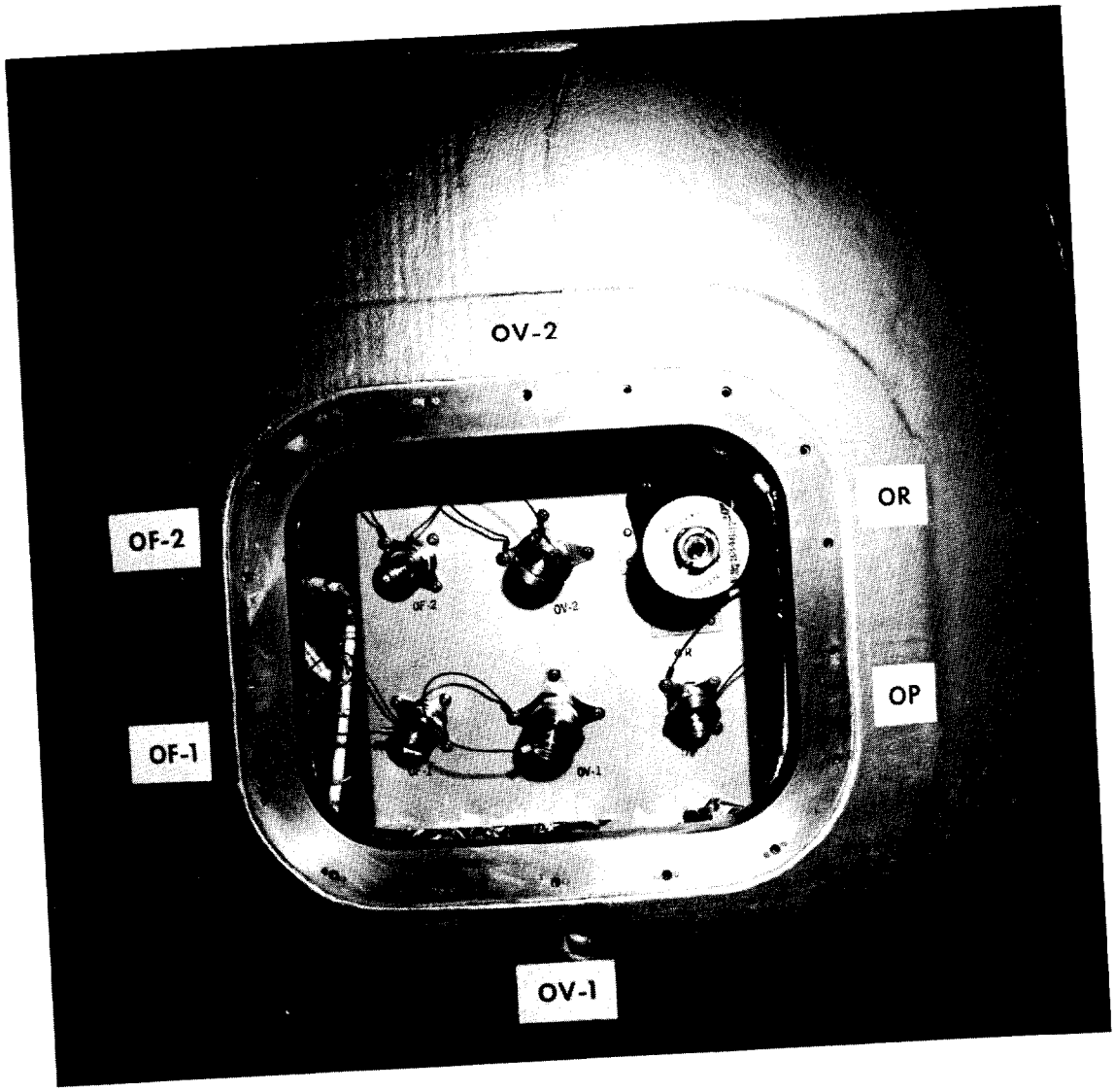

Figure D3-3.- SM oxygen system ground service panel.

their plumbing are identical except for one point in the feed line from tank no. 2, at which a ground service line tees into the feed line downstream of a check valve. This ground service line permits the operation of the fuel cells and the environmental control system (ECS) oxygen system from a ground source of oxygen without requiring the use of the flight tankage. This line terminates at the fitting designated OP in figure D3-3. The check valve prevents the pressurization of tank no. 2 from this ground source.

The pressure transducer, pressure switch, and relief valve are located in an oxygen system valve module external to the tank. A photograph of the module is shown in figure D3-4. Two of each of these components plus the check valve for tank no. 2 referred to in the previous paragraph comprise the module. Figure D3-4 shows the top of the oxygen shelf. There are approximately 19 feet of feed line from the tank pressure vessel to the valve module.

The feed line exits the oxygen system valve module and branches, one going to the ECS and the other to the fuel cell valve module where the lines from tanks no. 1 and no. 2 are manifolded within the body of this assembly. This module contains the check valves at the feed line entrance points and three solenoid shutoff valves, one for each of the fuel cells.

The cryogenic oxygen electrical system consists of the following items for each tank:

1. Two electrical heaters, rated at 77.5 watts each, 28 V dc. For ground operation, the heaters are rated at 415 watts each, 65 V dc. Four wires exit the tank connector. The wiring of the heater leads at the pressure control assembly is such that the two heaters are connected in parallel to a single power source. Power to the tank no. 2 heaters is provided from main bus B through a circuit breaker and through an on-off automatic switch. Automatic operation is provided through the pressure control assembly actuated by the pressure switches. The control logic requires that both oxygen tank pressure switches be below the low set-point to energize the heaters. Either switch sensing pressure above the high set-point will deenergize the heaters.

2. Two motor-driven fans rated at 28.4 watts each (three-phase, 200/115 V ac). Eight wires, one for each of the three power phases plus a neutral for each motor, exit the tank at the tank connector. They proceed to a fuse box assembly where each of the leads (except for the grounded neutrals) is individually fused by a 1-ampere fuse. Upon leaving the fuses, the leads from like phases of the two motors as well as the neutrals are joined within the fuse box, and four wires leave this assembly. The three power leads then pass through individual switch contacts and thence to individual circuit breakers. Each breaker is rated at 2 amperes. The fans can be operated in either a manual or automatic mode.

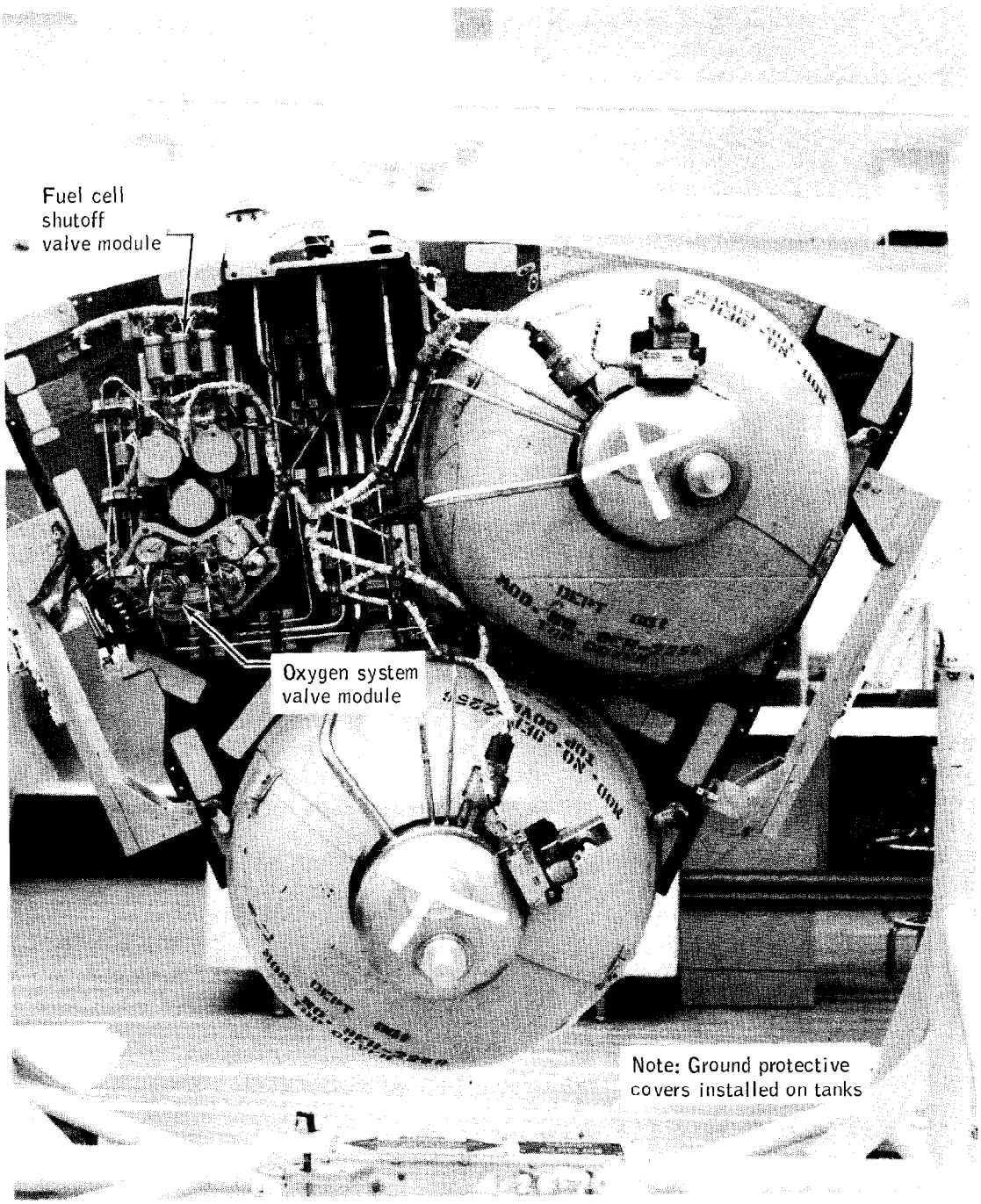

Figure D3-4.- Plan view of the top of the oxygen shelf.

3. A temperature sensor, a platinum resistance thermometer encased in an Inconel sheath. It is attached to the outside of the quantity probe. The resistance of the thermometer and consequently the voltage drop across the unit changes with temperature. The signal conditioner which serves as the reference voltage generator and amplifier is located on the oxygen shelf and its input to the resistor is current-limited to a maximum of 1.1 milliamperes. Four wires exit the tank connector and are connected to the signal conditioner. The signal conditioner is powered from ac bus 2 through a circuit breaker as a parallel load with the quantity gage signal conditioner. Additional description is provided in Appendix B.

4. A quantity gage, a capacitor consisting of two concentric aluminum tubes submerged in the oxygen. The dielectric constant of the oxygen, and consequently the measured capacitance, changes in proportion to its density. The signal conditioner, which serves as the reference voltage generator, rectifier, and amplifier, is located on the oxygen shelf. Two wires exit the tank connector and are connected to the signal conditioner. The signal conditioner is powered from ac bus 2 through a circuit breaker as a parallel load with the temperature sensor signal conditioner. Additional description is provided in Appendix B.

5. A vac-ion pump assembly, attached to the dome of the tank, is used only in prelaunch activities to maintain the tank annulus at the required vacuum level. The pump functions by bombarding a titanium cathode with ionized gas molecules and ion pumping results from the gettering action of sputtered titanium particles. The high-voltage power supply of the pump is an integral part of the pump assembly. Leads for the vac-ion pump do not penetrate the pressure vessel and the pump is not normally powered in flight.

ELECTRICAL SYSTEM CONFIGURATION AT TIME OF ACCIDENT

The electrical power system, in general, provides multiple power busses with switching options for selecting an operating configuration. At 55:53:21, the electrical system was configured in accordance with reference 1, as shown in figure D3-5, with fuel cells 1 and 2 connected to main bus A and fuel cell 3 connected to main bus B. Inverter 1 was connected to main bus A and powering ac bus 1. Inverter 2 was connected to main bus B and powering ac bus 2. Inverter 3 was not connected. Battery busses A and B were not connected to main bus A or B. The switches controlling heater operation for both oxygen tanks were in the "automatic" position, controlling heater operation through the pressure control assembly. Pressures in the oxygen tanks were at levels which did not demand operation of the heaters. Temperature and quantity sensors on oxygen tank no. 2 were energized from ac bus 2. The quantity gage

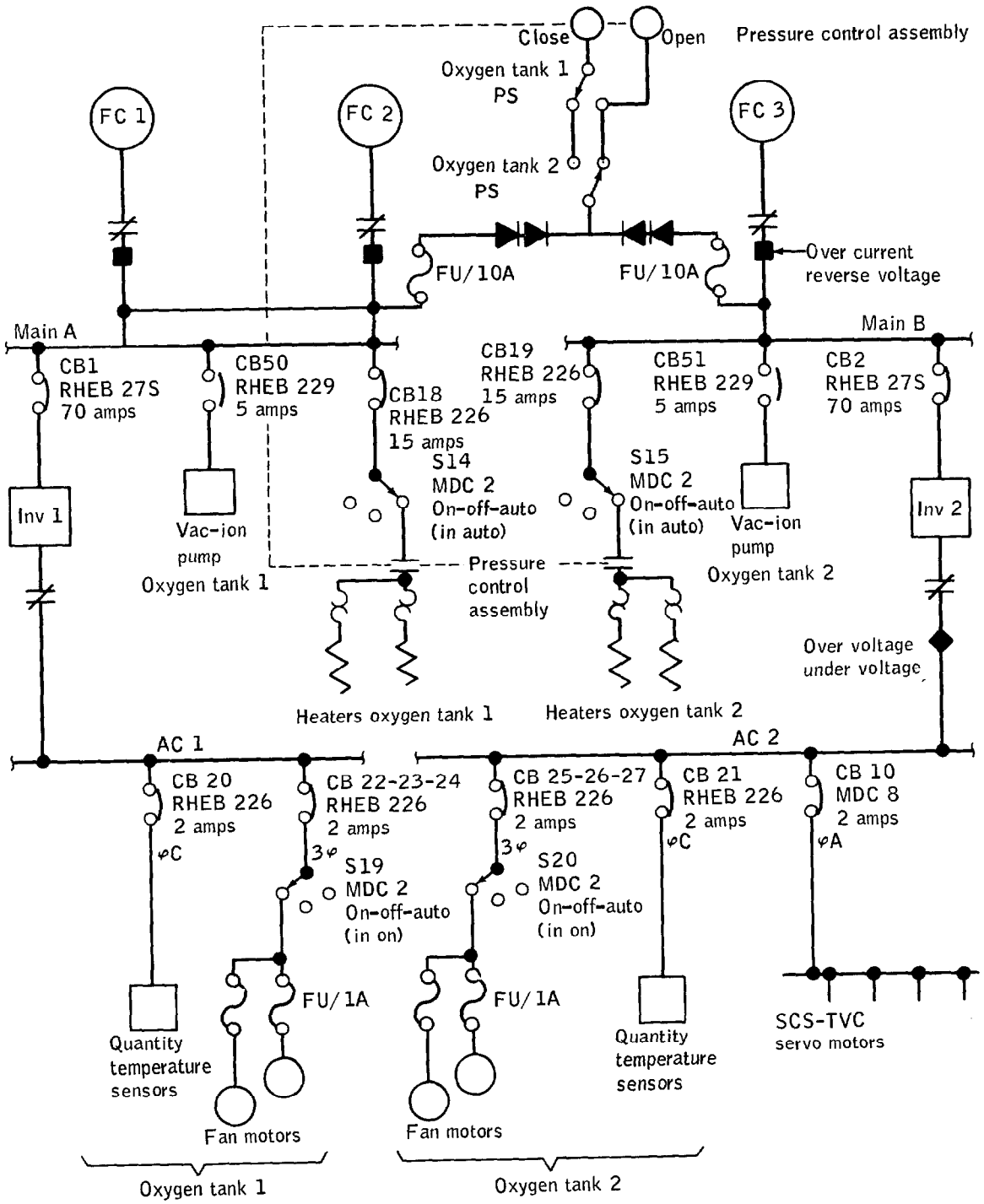

Figure D3-5.- Electrical schematic of relevant portions of electrical power system at 55:53:21.

had remained off-scale high from 46:40:06, indicating a probable short circuit either on the leads or the probe assembly. Operation of the fan motors in the oxygen tanks was accomplished throughout the mission using manual control in lieu of the automatic operation afforded by the logic of the pressure control assembly. A routine operation of the fans was requested by the ground at 55:52:58 and acknowledged by the crew at 55:53:06. Energizing of the fans in oxygen tank no. 1 is confirmed by a drop in voltage of ac bus 1 and an increase in total fuel cell current at 55:53:18. Energizing of the fans in oxygen tank no. 2 is confirmed by a drop in voltage of ac bus 2 and an increase in total fuel cell current at 55:53:20. Data substantiating operation and operation times are presented in Appendix B.

STRUCTURAL EVALUATION OF THE OXYGEN TANK

The oxygen tank consists of two concentric shells, an inner shell (the pressure vessel) and an outer shell (fig. D3-6). The space between the two shells is evacuated during normal operation and contains the thermal insulation system, fluid lines, and the conduit which houses all of the electrical wires entering the pressure vessel.

The oxygen tank is discussed from the standpoint of materials, processing, welding, qualification program, stress levels, fracture analysis, and environmental testing.

Materials, Processing, and Welding

Inner shell.- The pressure vessel is made from Inconel 718, a precipitation hardenable nickel base alloy having good strength, ductility, and corrosion resistance over the range of temperatures from -300° F to above 1400° F. The nominal composition of Inconel 718 is 19 percent chromium, 17 percent iron, 0.8 percent titanium, 5 percent columbium, 0.6 percent aluminum, and the remainder nickel. The heat treatment specified for Inconel 718 for this application was the following:

Hold at 1800° F ± 25° F for 1 hour

Air cool to 1325 ± 25° F and hold for 8 hours

Furnace cool to 1150° F and hold for 8 hours

Air cool

This treatment should produce typical ultimate tensile strength of 198,000 psi and yield strength of 170,000 psi at 70° F. Ultimate and

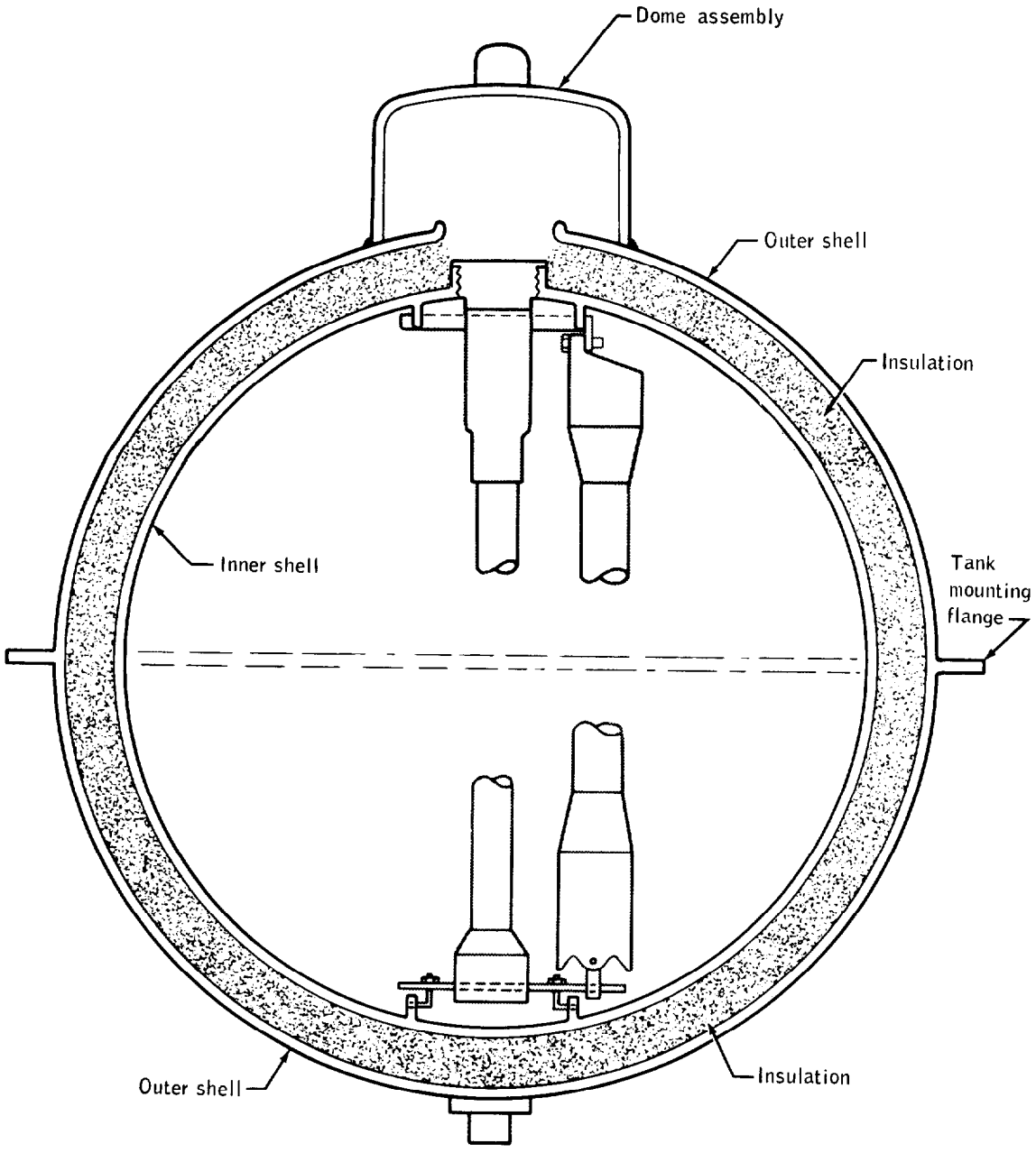

Figure D3-6.- Oxygen pressure vessel schematic.

yield-strength values increase with decreasing temperature and reach 228,000 psi and 189,000 psi, respectively, at -190° F. These values exceed those assumed in the design of the vessel, which were 180,000 psi ultimate tensile strength and 150,000 psi yield strength at room temperature (ref. 2). After burst tests, tensile specimens were cut from test vessels PV-1 and PV-4, and strength measurements were made at room temperature. Each specimen exceeded minimum requirements.

Inconel 718 is considered to be an excellent selection for use at the temperatures required by this design and when properly cleaned is compatible with liquid oxygen.

The pressure vessel is made by electron beam welding two hemispheres at a weld land (fig. D3-7) that is 0.139 ± 0.002 inch thick. The weld land is faired to a membrane of 0.059-inch thickness over a distance of about 2 inches. Cameron Iron Works, Inc., forges the hemispheres to a wall thickness of 0.75 inch, and applies the complete heat treatment. The hemispheres are X-rayed following forging. The Airite Company machines the hemispheres to dimension and welds them together from the outside. First, an intermittent tack weld pass is made, followed by a complete tack weld. The third pass provides complete penetration, and a fourth pass penetrates about one-third of the thickness. Finally, a cover pass is made. Figure D3-8 illustrates the welding sequence. The weldments are X-rayed and dye-penetrant inspected from the outside. Inspection of the inside of the pressure vessel is by visual means only and dye penetrant is not used. Use of one of the available liquid-oxygen-compatible dye penetrants would enhance the detection of cracks or similar weld defects inside the vessel.

The literature has very little data on electron-beam welding of Inconel 718. However, it is frequently used in the aerospace industry and there is no reason to question the practice in this instance. One potential problem sometimes found when this nickel-base alloy is welded is micro-fissuring in the heat-affected zone. Such fissures either do not propagate to the surface, or are very difficult to detect. Unfortunately, high-contrast X-rays of this material are difficult to obtain, particularly in the configuration of this tank. No evidence of a weld cracking problem has been found in the manufacture of these pressure vessels. Thus there is no justification for postulating that micro-fissuring was a factor in the accident being investigated.

A total of 39 data packages on oxygen pressure vessels were reviewed and it was ascertained that only 12 vessels had had weld discrepancies. Table D3-1 describes the weld discrepancies and their disposition. Neither of the two Apollo 13 oxygen tanks flown (S/N 10024XTA0008 and S/N 10024XTA0009) appear on this list. There were no recorded weld discrepancies during the manufacture of these tanks.

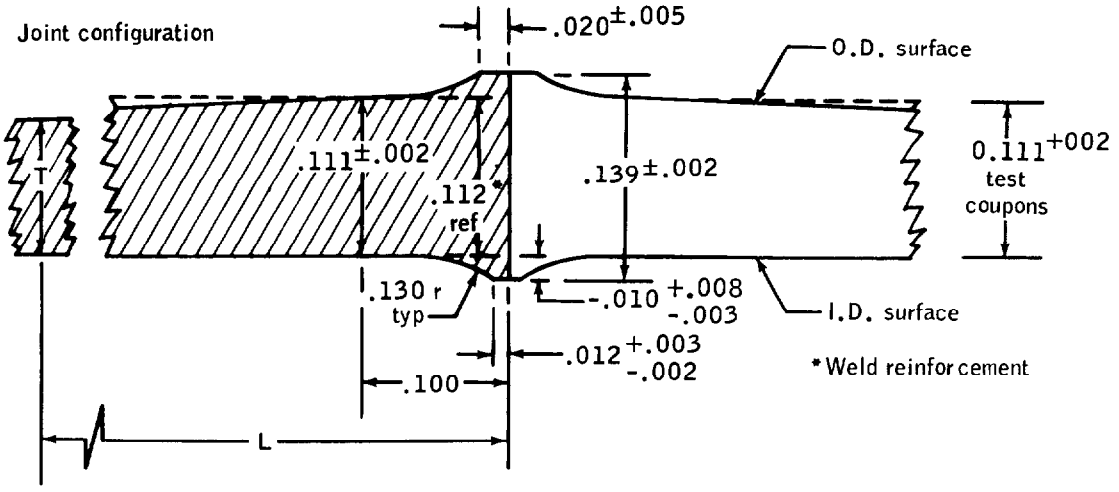

P/M thickness L	T	Tank radius O.D.	Dimensions I.D.	
1.000	.084 ±.002	14.808 ref_{arc}	12.528 +005 -0	Sph rad
2.000	.067 ±.002	14.808 ref_{arc}	12.528 +005 -0	Sph rad
3.000	.059 + 004 - 000	12.587 ref_{arc}	12.528 +005 -0	Sph rad

Weld schedule (Electron beam weld)

Parameter	Pass sequence 1-tack	2-seal	3-pene.1	4-pene.2	5-cover
Voltage - Kv	80	80	115	95	85
Amperes - MA	1.5	1.5	6.0	4.0	3.0
Beam deflection - in.	0.012	0.012	.024/.036	.040/.080	0.110
Travel - in./min	18	→	→	→	→
Vacuum - mm hg	2×10^{-4}	→	→	→	→

Notes: (1) 0.002" gap, 0.003" offset (max typ)
(2) No weld repairs allowed
(3) Typical weld sequence shown on attached sketch

Figure D3-7.- Girth weld joint configuration and schedule.

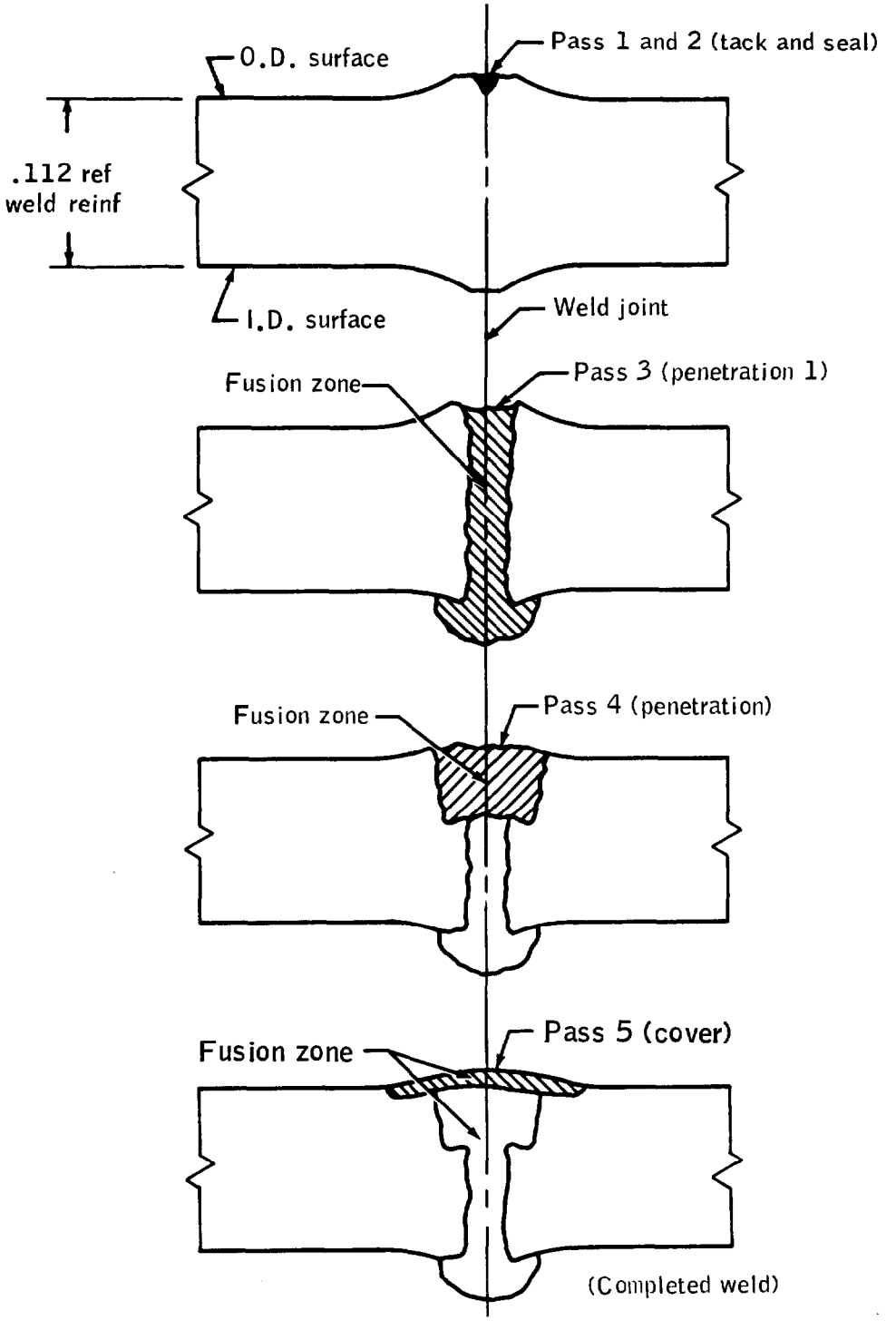

Figure D3-8.- Weld sequence.

TABLE D3-I.- AIRITE PRESSURE VESSEL WELD DISCREPANCIES

Serial no.	Spacecraft	Discrepancy
XTA0005	101	Weld bead 0.005 inch concave by 0.600-inch length. Remainder undercut 0.002 inch below weld land parent metal. Accepted based upon X-ray and comparison to qual. unit used in burst. Beech MRR.
XTA0010	103	Undercut below weld land in one area 0.0015 inch deep by 0.750 inch length adjacent to upper hemisphere. Due to heavy weld drop-through. Accepted for unrestricted use by NR MRD.
XTA0013	106	Hemisphere dimensional characteristics resulted in excessive weld mismatch. Units were successfully welded after NR MRD. Finished vessel met all requirements.
XTA0016	107	Four areas of concavity in center of weld bead: no. 1, 0.0025 inch depth; no. 2, 0.0055 inch depth; no. 3, 0.0045 inch depth; no. 4, 0.0025 inch depth. Concavity due to excessive drop-through. Rewelded using two 360-degree weld passes in accordance with NR MRD. After rework of above, three areas of concavity remained: no. 1, 0.0025 inch below parent metal; no. 2, 0.004 inch below parent metal; no. 3, 0.0015 inch below parent metal. Warpage occurred due to lack of constraint. Accepted for unrestricted usage per NR MRD based upon positive margins of safety.
XTA0022	110	Borescope showed entire weld land visible and not consumed through 360-degree circumference due to lack of penetration. Rewelded per NR MRD instructions.
XTA0017	110	Borescope revealed lack of drop-through in an area 1/2 inch in length. Rewelded by one 360-degree pass per NR MRD. Edge of weld on upper hemisphere undercut from 0.001 inch to 0.003 inch into parent material for 360 degrees following rewelding per above--reworked and accepted by NR MRD based upon stress analysis.

TABLE D3-I.- AIRITE PRESSURE VESSEL WELD DISCREPANCIES - Concluded

Serial no.	Spacecraft	Discrepancy
XTA0024	111	Hemisphere dimensional characteristics out of specification. Units successfully welded after certification test specimens duplicating conditions were acceptable. Discrepancies were consumed during welding. Beech MRR.
XTA0021	111	Incomplete weld penetration for a distance of 17-3/8 inches. Rewelded per NR MRD.
XTA0033	Unassigned	Upper hemisphere dimensions out of specification. Accepted for welding with fit up with another hemisphere. Beech MRR.
XTA0019	Unassigned	Borescope revealed complete weld land (0.012 inch) still visible--repair welded per NR MRD.
XTA0003	Unassigned	Borescope and X-ray revealed incomplete penetration major distance of weld. Rewelded per Airite procedure. Beech MRR. Weld concavity from 0.001 to 0.0055 inch deep on drop-through side of weld on upper hemisphere. Maximum width is 0.003 inch--accepted for unrestricted use by NR MRD.
XTA0032	Unassigned	Borescope revealed area approximately 0.600 inch long with incomplete consumption of weld lands. X-ray indicated complete penetration. Rewelded by Airite procedure. Beech MRR.

Outer shell.- The outer shell is made of Inconel 750, also a nickel base alloy having the following nominal composition: 15 percent chromium, 7 percent iron, 2.5 percent titanium, 1 percent columbium, 0.7 percent aluminum, and the remainder nickel. According to references 3 and 4, the outer shell can be annealed. Typical strength values for the annealed alloy are 130,000 psi ultimate strength and 60,000 psi yield strength. This is more than adequate for this application. The wall thickness of the outer shell is 0.020 ± 0.002 inch. When the space between the two shells is evacuated, the outer shell preloads the insulation between the two shells. The dome of the outer shell contains a burst disc designed to vent the space between the shells to ambient pressure at a pressure differential of 75 ± 7.5 psi.

Cryogenic tank tubing.- Three fluid lines (fill line, vent line, and feed line), and an electrical conduit are fusion welded to the close-out cap (tube adapter) that is screwed into the top of the pressure vessel. The cap is secured to the pressure vessel by a circumferential seal weld. The four lines are made of Inconel 750, annealed Aerospace Materials Specification (AMS) 5582. The tubes traverse the space between the two shells and exit the outer shell at the side of the tank coil cover. The nominal strength of the annealed tubing is 140,000 psi ultimate, and 80,000 psi yields, which is more than adequate for the application, as the stress level in the tubing is only about 17,000 psi.

After the tubes are welded to the cap, a visual inspection, helium leak test (3 psi), and proof-pressure tests are used to assess the quality of these welds (ref. 5). This is reasonable because of the low stress levels involved. Liquid-oxygen-compatible dye penetrant inspection and subsequent cleaning would enhance the possibility of finding surface cracks. X-rays of these welds would be difficult to obtain and should be of dubious value.

The four lines extend only a few inches from the tank dome. When the tank is assembled on the oxygen subsystem shelf, the fluid tubes are joined by brazing to the 304L annealed corrosion resistant steel tubes of the spacecraft systems. Although joining Inconel 750 and 304L steel constitutes a bimetallic couple, it is satisfactory in this application because of the dry environment that is maintained.

Qualification Program

The pressure vessel qualification program was conducted by Beech Aircraft Corporation. Four pressure vessels were subjected to burst tests as described in references 6 through 12.

Prior to each burst test, the vessel was subjected to an acceptance pressure test at 1357 psig and checks were made for leaks. No leaks were

observed in any of the vessels. In Appendix F of reference 9, there is an analysis of the proof test of vessel PV-4. The following table lists some of the strain gage readings taken during the qualification testing.

MEASURED STRESS LEVELS IN KSI

Tank	Internal pressure, psig	2.8 inches from upper pole	2.0 inches from girth weld	Lower pole area	Membrane (0.061-inch thick)
Tank PV-4 70° F	1020 1357	108.3[a] 139.7[b]	106.1 139.4	97.7 128.9	105.8 -
Tank PV-1 -320° F	1020	116.7	113	-	-

[a]Design value 110 ksi

[b]Design value 145 ksi

For the cryogenic burst tests, the vessels were filled with liquid nitrogen and placed in an open dewar of liquid nitrogen. The ambient temperature burst tests used water as the pressuring medium. The burst pressures of the qualification vessels were as follows:

Tank	Test condition	Burst pressure, psig
PV-1	Cryogenic (LN_2, -320° F)	2233
PV-2	Cryogenic (LN_2, -320° F)	2235
PV-3	Ambient temperature (70° F)	1873
PV-4	Ambient temperature (70° F)	1922

All ruptures were similar; the failures apparently started about 2 or 3 inches from the pole of the tank on the top at the transition from the heavier section to the membrane section. The fractures progressed around the boss area, proceeded essentially perpendicular to the girth weld, and then crossed the girth weld in both ambient tests and in one of the cryogenic tests. In the other cryogenic temperature test vessel, a large fragment came out of the upper hemisphere. In no case was there violent fragmentation. After the burst of PV-1 at 2233 psig, initial failure was judged to have occurred at the end of the neck taper around the top pole. The rupture progressed downward, branching into a Y. After coming into contact with the weld, the rupture followed the weld fusion zone.

The following is a quotation from reference 9:

"2.3.7 Conclusions - Based on the above analysis and evaluation, the following conclusions are made:

(1) Burst failure initiated at the end of the boss taper in the upper hemisphere and resulted from plastic deformation beyond the tensile strength of the base material at ambient temperature.

(2) Rupture was of a hydrostatic type.

(3) The appearance of all failed areas was judged to indicate good ductility of the base metal and weldments.

(4) No significant mismatch was observed on the specimens investigated.

(5) All fractures across the weld were shear fractures and of a secondary nature.

(6) The grain size throughout the vessel was fine (ASTM-5 to 8) and relatively equiaxed.

(7) The ambient burst test was judged to be completely successful by Beech Aircraft Corporation Engineering, and the results of the test indicate approximately 100 percent efficiency for the material at the test temperature."

The data from these pressure vessel tests satisfy the qualification requirement for an ultimate factor of safety of 1.5 at ambient temperature with adequate margins.

In 1967 North American Rockwell verified analytically the structural integrity of the oxygen tank (ref. 13). An MSC structural analysis report (ref. 14), also issued in 1967, confirmed the structural integrity of these tanks and compared the analysis with the results of the burst tests. This comparison showed good correlation between analytical and test results. The MSC calculations were based on minimum guaranteed sheet thicknesses and minimum material properties. Even better correlation is obtained by using the actual thicknesses and material properties of the test items.

These analyses show the maximum stresses in the tank during pressurization to be in the upper spherical shell at the transition from the constant thickness shell to the thickened area adjacent to the penetration port. Actual stresses determined from strain gage readings during burst tests are consistent with the analyses.

FRACTURE MECHANICS

The design of the supercritical oxygen tank was based on conventional elastic stress analysis which assumes a homogenous material and uses the conventional tensile properties for the calculation of safety factors. In reality, all fabricated materials contain crack-like flaws which may be associated with weld defects or with metallurgical segregations which can transmit only negligible loads across their boundaries. The load-carrying capacity of high-strength materials, particularly in thick sections, may be severely reduced by the presence of even small flaws which can trigger a brittle catastrophic failure at loads well below those considered safe by conventional design procedures. Furthermore, in many cases the type of flaw present cannot be found by nondestructive inspection techniques and, for this reason, a proof test must be depended upon to identify those structures which might fail in service.

At the outset it should be appreciated that linear elastic fracture mechanics and the associated American Society of Testing Materials (ASTM) Standard Method of Test for Plane Strain Fracture Toughness, K_{Ic}, are not directly applicable to an analysis of the fracture of the oxygen pressure vessel material in the thicknesses employed, or for that matter in very much larger thicknesses. The evidence for this lies in early results from a fracture test program now underway at Boeing. These results indicate that specimens containing deep cracks in parent metal, or in electron beam weld metal representative of the oxygen pressure vessel, fail at net stresses very close to or slightly above the corresponding yield strength whether they are tested at 70° F or -190° F. While the plane strain fracture toughness, K_{Ic}, cannot be determined from the data available, a lower bound estimate may be made from test results reported on 2-3/4 inch diameter notched round bar specimens (ref. 15). These large specimens were cut from forgings of Inconel 718 and tested at -110° F. The corresponding yield strength was about 172 ksi and the notch strength was 40 percent above the yield strength. Formal calculations give an "apparent K_{Ic}" value of 190 ksi $-\sqrt{\text{in.}}$ which may be taken as a lower bound for a yield strength of 172 ksi. This is approximately equal to the 70° F parent metal yield strength of the oxygen pressure vessel. Properly made electron beam weldments should have at least this

high a K_{Ic} value since they are not heat treated after welding and therefore have a lower yield strength than the parent metal. At -190° F the yield strength of the parent and weld metal will increase about 10 percent; however, for this austenitic alloy the corresponding change in toughness would be expected to be negligible.

Failure Modes

While "apparent K_{Ic}" values should not be used to develop relations between tank wall stress and critical flaw size, the lower bound value of K_{Ic} can be used to show that the pressure vessel would not fail in a brittle manner. When the parameter β_{Ic}, the ratio of crack tip plastic zone size factor to specimen thickness, is greater than 1-1/2, brittle fracture is very unlikely. This parameter is given by

$$\beta_{Ic} = \frac{1}{B} \frac{K_{Ic}^2}{F_{ty}^2}$$

For the oxygen tank B the effective weld land thickness after welding is 0.111 inch; the yield strength of the weld F_{ty} is 110 ksi at -190° F (table D3-II), and the lower bound of K_{Ic} is 190 ksi $\sqrt{\text{in.}}$.

TABLE D3-II.- TYPICAL PARENT METAL AND WELD TENSILE PROPERTIES[a]

Temperature, ° F	Parent metal		Weld metal	
	F_{tu} - ksi	F_{ty} - ksi	F_{tu} - ksi	F_{ty} - ksi
-190	228	189	187	[b]110
70	198	170	158	100

[a]Determined by Boeing on Inconel 718 forgings using same heat treatment given the oxygen pressure vessel and on electron beam weldments given no heat treatment.

[b]Gage length equal to weld width.

Using these values, $\beta_{Ic} = 27$. A similar calculation for the parent metal in the membrane yields $\beta_{Ic} = 16$. On this basis, the mode of failure of the pressure vessel would be expected to be ductile tearing rather than shattering. However, it is not known whether this mode would lead to a stable through-thickness crack, and a consequent slow leak into the space between the pressure vessel and the outer shell, or to a rapid tearing fracture with consequent destruction of the outer shell and the quick release of a large volume of oxygen. Which of these two possibilities is most likely depends in part on the flaw size giving rise to the final fracture and on the rate of depressurization as compared with the rate of crack propagation. To settle this matter would require burst tests on intentionally flawed tanks.

If a local area of the pressure vessel wall or the tube adapter were heated to a sufficiently high temperature by some internal or external source, the tank would blow out at this local area. According to data furnished by Boeing under contract to NASA, the strength of Inconel 718 would degrade rapidly if the metal temperature exceeded about 1200° F. At 1400° F the tensile strength would be about 50 percent of the room temperature value, and at 1600° F would be less than 30 percent of this value. At a tank pressure of 1008 psi, the parent metal wall stress based on membrane theory is about 108 ksi. A ductile rupture at this stress would likely occur if the tank were at a uniform temperature of 1400° F. The restraining effect of the cool surrounding metal would raise the temperature required for a local blowout and this situation is best evaluated by suitable experiments.

Effectiveness of the Proof Test

The proof test is the last, and should be the best, flaw detection procedure applied to a pressure vessel. Ideally, the proof test should cause failure if there are any flaws present that could grow to a critical size during subsequent pressurization. For the oxygen tanks in question, a fracture mechanics analysis cannot be made to assess the adequacy of the proof test because of the high toughness of the material and the thin sections used. These factors in themselves, of course, contribute to the confidence that can be placed in the integrity of the pressure vessel and, as discussed in the previous section, essentially rule out the possibility of brittle failure. However, it is worthwhile to estimate the effectiveness of the proof test in identifying those pressure vessels which might develop leaks during pressure cycles subsequent to proof. The failure model proposed considers the plastic instability fracture of a ligament of material produced by incomplete fusion during electron beam welding. The main features of this model are illustrated in figure D3-9. It essentially represents a long flaw in the tank wall at the

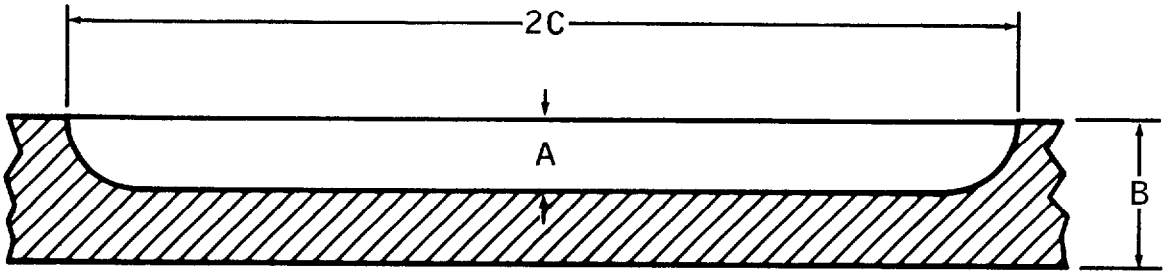

Area of lack of fusion produces
an effective crack of depth A
& length 2C in tank wall of
thickness B. 2C >> A

Figure D3-9.- Ligament model for ductile fracture of pressure vessel.

equatorial weld. It is postulated that the ligament will fail when its stress reaches the tensile strength of the material. Calculations show that the ligament stress σ_ℓ is related to the average wall stress σ_g as follows:

$$\sigma_\ell = \sigma_g \frac{B}{B - A}$$

where the dimensions are defined in figure D3-9. The maximum relative flaw depth that can be sustained without failure is then

$$\frac{A}{B} = 1 - \frac{\sigma_g}{F_{tu}} \qquad (1)$$

where F_{tu} is the ultimate tensile strength. Failure will occur by tearing of the ligament accompanied by rapid decompression of the tank. It should be appreciated that this is a rather crude model of ductile fracture, and will probably overestimate the failure stresses in a spherical vessel. However, it should be useful in assessing the effectiveness of the proof tests in light of subsequent service, because of the very large margins between proof and operating pressures.

The pressure cycles applied to the Apollo 13 oxygen tank no. 2 are shown in table D3-III. It should be noted that the oxygen tank no. 2 had several extra pressure cycles in addition to those normally applied. These were associated with rechecks for heat leaks and with the "shelf drop" incident. The additional cycles do not affect this analysis nor should they have reduced the integrity of the tank during mission service.

The ratio of tank pressures necessary to cause ligament failure for a given relative flaw size A/B at two temperatures will be equal to the ratio of the tensile strength of the material at these temperatures. On this basis, the maximum flaw size that could exist before CDDT is established by the last high pressure helium proof specified as $1260 \begin{smallmatrix}+50\\-0\end{smallmatrix}$ psi at ambient temperature (1276 psi for oxygen tank no. 2). From equation (1), the corresponding value of A/B for the weld metal is 0.55, based on a weld tensile strength of 158 ksi at room temperature, a weld land thickness of about 0.111 inch, and a nominal weld land stress of 71 ksi.

The question now arises as to whether a flaw of this size could propogate through the wall during subsequent pressurization and produce a leak. Flaw growth could occur by sustained loads or cyclic loads. In the absence of an aggressive environment, it is generally recognized that sustained load flaw growth will not occur at loads less than 90 percent of that necessary to produce failure in a continuously rising

TABLE D3-III.- HISTORY OF PRESSURE CYCLES APPLIED TO APOLLO 13
SUPERCRITICAL OXYGEN TANK NO. 2

[Record from North American Rockwell Space Division]

Organization	Test media	Date	Peak pressure, psi (a), (b)	Time, hr:min	Test name
Beech	H_2O + He	6-20-66	1336	00:24	Pressure vessel, acceptance
Beech	GN_2	7-15-66	1340	00:56	Internal leak check on complete assembly
Beech	LN_2	7-15-66	920	00:51	Cold shock
Beech	GN_2	9-15-66	[c]1333	00:54	Internal leak check
Beech	LN_2	9-15-66	[c]918	00:51	Cold shock
Beech	Helium	10-19-66	1303	09:49	Proof and leak
Beech	Helium	10-19-66	888	01:00	Proof and leak
Beech	LOX	12-20-66	1333	40:05	dq/dm
Beech	LOX	10-24-66	922	25:04	dq/dm
Beech	Helium	1-31-67	[c]1305	09:07	Proof and leak
Beech	LOX	2- 2-67	[c]1321	28:39	dq/dm
Beech	LOX	2- 3-67	[c]920	22:16	dq/dm
NAR-SD	Helium	4-29-68	1262	06:45	Leak
NAR-SD	Helium	5- 1-68	1002	01:00	Leak
NAR-SD	Helium	5- 1-68	968	13:13	Leak
NAR-SD	Helium	5- 2-68	1104	08:02	Leak
NAR-SD	Helium	5-27-68	[c,d]1262	02:54	Leak
NAR-SD	Helium	5-28-68	[c]1102	01:07	Leak
NAR-SD	Helium	11-18-68	[d]1276	02:24	Leak
NAR-SD	Helium	11-18-68	1002	01:40	Leak
NAR-SD	Helium	7-17-69	1025	01:39	Leak
NAR-SD	LOX	4- 9-70	925	43:53	Launch loading

[a] Pressure cycles below 400 psi not recorded
[b] It could not be determined whether pressure measurements represented psia or psig
[c] Pressure cycles not normally applied
[d] $1260\ ^{+50}_{-\ 0}$ psi specification

load test. Following the 1276 psi helium proof test, no subsequent pressurization exceeds 85 percent of this pressure, and consequently sustained load flaw growth is extremely unlikely. Confidence in this conclusion can be obtained from the test results of a Boeing program now underway. These results apply to specimens containing small but deep cracks in both parent metal and electron beam weld metal of Inconel 718 forgings heat treated in the same way as the oxygen tank material. The early data show no crack growth in 20 hours at -190° F for specimens subjected to 160 percent of the nominal operating stress.

Cyclic loads during the flight operation would be caused by cyclic operation of the heaters (about once per one-half hour). The associated pressure cycles are very small with a minimum-to-maximum stress ratio of about 0.93. Flaw growth due to these small cyclic loads is considered extremely unlikely during the mission for the following reason: maximum nominal operating stress in the weld land (at 935 psi) is about 28 percent of the weld tensile strength at -190° F. Therefore, with a flaw size of A/B = 0.55, the ligament stress would be only about 63 percent of the weld tensile strength. On the basis of the known fatigue behavior of Inconel 718 welds (ref. 16), it would be expected that ligament failure due to cyclic loads induced by heater operation would not be a consideration until hundreds of cycles had been accumulated. Confidence in this conclusion can be obtained from the early results of the previously mentioned on-going Boeing program. These results indicate that parent and electron beam weld metal specimens of Inconel 718 containing small but deep cracks do not show crack growth at -190° F after 15,000 cycles at minimum-to-maximum stress ratio of 0.95 and a mean stress of about 170 percent of the nominal operating value.

While the conclusions based on the ligament model are consistent with the Boeing data obtained from specimens with small flaws, these test results cannot be used to prove the validity of the model because it applies to large flaws. Therefore, it is planned to check the conclusions reached on the basis of this model by testing specimens at MSC which will contain large, deep cracks. Specimens of both electron beam welds and parent metal will be subjected at -190° F to the mean and cyclic stresses encountered in flight operation of the oxygen tank.

In assessing the effectiveness of the proof test, no consideration was given to the possibility of failure in regions remote from the welds (e.g., the main membrane or neck of the vessel). Conventional stress analysis (ref. 14) shows that the highest stresses occur in the transition region between the weld lands and the uniform thickness membrane. Stresses in the neck region are very low and comparable to those in the weld land. The ligament model is not applicable to these regions of the vessel remote from the weld since there is no clear mechanism by which a large flaw could be introduced into the parent metal. Experience shows that